Timing of the first drainage of the Baltic Ice Lake synchronous with the onset of Greenland Stadial 1

Article

Accepted Version

www.reading.ac.uk/centaur

CentAUR

1 **Timing of the first drainage of the Baltic Ice Lake synchronous**

2 **with the onset of Greenland Stadial 1**

3 FRANCESCO MUSCHITIELLO, JAMES M. LEA, SARAH L. GREENWOOD, FAEZEH M. NICK,

4 LARS BRUNNBERG, ALISON MACLEOD AND BARBARA WOHLFARTH

8   Glacial varves can give significant insights into recession and melting rates of decaying

9   ice sheets. Moreover, varve chronologies can provide an independent means of

10   comparison to other annually resolved climatic archives, which ultimately help to

11   assess the timing and response of an ice sheet to changes across rapid climate

12   transitions. Here we report a composite 1257-year long varve chronology from south-

13   eastern Sweden spanning the regional late Allerød-late Younger Dryas pollen zone.

14   The chronology was correlated to the Greenland Ice Core Chronology 2005 using the

15   time-synchronous Vedde Ash volcanic marker, which can be found in both

16   successions. For the first time, this enables secure placement of the Lateglacial

17   Swedish varve chronology in absolute time. Geochemical analysis from new varve

18   successions indicate a marked change in sedimentation regime accompanied by an

19   interruption of ice-rafted debris deposition synchronous with the onset of Greenland

20   Stadial 1 (GS-1; 12 846 years before 1950 AD). With the support of a simple ice

21   flow/calving model, we suggest that slowdown of sediment transfer can be explained

22   by ice-sheet margin stabilisation/advance in response to a significant drop of the Baltic

23   Ice Lake level. A reassessment of chronological evidence from central-western and

24   southern Sweden further supports the hypothesis of synchronicity between the first

25   (penultimate) catastrophic drainage of the Baltic Ice Lake and the start of GS-1 in

26   Greenland ice cores. Our results may therefore provide the first chronologically robust

27   evidence linking continental meltwater forcing to rapid atmosphere-ocean circulation

28   changes in the North Atlantic.

29   *Francesco Muschitiello (Francesco.muschitiello@geo.su.se), Sarah L. Greenwood and*

30   *Barbara Wohlfarth, Department of Geological Sciences and Bolin Centre for Climate*

31 *Research, Stockholm University, SE-10691, Stockholm, Sweden; James M. Lea and Lars*

32 *Brunnberg, Department of Physical Geography and Bolin Centre for Climate Research,*

33 *Stockholm University, SE-10691, Stockholm, Sweden; Faezeh M. Nick, Department of*

34 *Geology, University Centre in Svalbard (UNIS), PO Box 156, NO-9171 Longyearbyen,*

35 *Norway, Centre for Ice and Climate, Niels Bohr Institute, University of Copenhagen,*

36 *2100 Copenhagen, Denmark; Alison MacLeod, Department of Geography, Royal*

37 *Holloway University of London, Egham, Surrey TW20 0EX, UK.*

38 Understanding the timing and interplay between past ice-sheet dynamics and abrupt

39 climate change can be significantly enhanced where suitable highly resolved and

40 independently dated palaeoenvironmental archives are available. Glacial varves are

41 such a proxy, providing an indirect record for ice-marginal dynamics at potentially

42 annual or sub-annual resolution. Furthermore, these records can provide lengthy and

43 continuous chronologies, which can be directly compared to other climate archives.

44 In turn, this allows the examination of potential couplings between changing regional

45 ice-sheet behaviour and climate change.

46 The Swedish glacial varve chronology or 'Swedish Time Scale' (STS) provides a

47 reconstruction preserving information regarding the dynamics and the melting of the

48 Fennoscandian Ice Sheet (FIS). It is therefore an ideal data set to investigate ice sheet

49 dynamics and sensitivity in response to climate change. The STS is based on visual

50 cross-correlation of more than 1000 ice-proximal clastic varve-thickness successions,

51 which reflect the seasonal sediment input associated with the deglaciation of Sweden

52 (De Geer 1912, 1940). These clastic varves, with their distinct silt dominated summer

53 and clay dominated winter layers were deposited in the ice-dammed Baltic basin, the

54   Baltic Ice Lake (BIL), and can today be found along the Baltic Sea coast and in the Baltic

55   Sea (Strömberg 1985; Cato 1987; Björck *et al.* 1992; Brunnberg 1995; Wohlfarth *et al.*

56   1994, 1995). The younger part of the STS is made up of postglacial delta sediments,

57   which were and still are deposited in the estuary of River Ångermanälven in northern

58   Sweden (Cato 1985, 1987, 1998; Wohlfarth *et al.* 1997). However, a putative gap of

59   700-900 varve years during the early and/or mid Holocene (Wohlfarth 1996;

60   Wohlfarth *et al.* 1997; Andrén *et al.* 1999), as well as difficulties in correlating varve

61   diagrams from Blekinge in southernmost Sweden to those of south-eastern Sweden

62   (Wohlfarth & Possnert 2000) has so far posed a challenge to establishing an absolute

63   and continuous varve chronology from present back to >14 000 varve years. Given

64   the chronological uncertainties due to missing varves, each regional varve chronology

65   thus stands on its own (Wohlfarth & Possnert, 2000).

66   The Lateglacial clay-varve diagrams from south-eastern Sweden (northern

67   Småland and Östergötland) (Kristiansson 1986; Brunnberg 1995; Wohlfarth *et al.*

68   1993, 1994, 1995, 1998), spanning the later part of the regional Allerød pollen zone

69   (AL) and the early part of the regional Younger Dryas pollen zone (YD), constitute one

70   of the most valuable portions of the STS. This Lateglacial varve chronology (LGC) is

71   built by visual cross-correlations and corroborated by statistical analysis (Holmquist &

72   Wohlfarth 1998), but is at present only tentatively linked to a calendar-year time scale

73   by means of ^{14}C dating (Goslar *et al.* 1999; Wohlfarth & Possnert, 2000).

74   The recent finding of the Vedde Ash in a glacial varve succession from the same

75   region (MacLeod *et al.* 2014) now offers an excellent opportunity to secure the

76   floating LGC chronology to an absolute time scale, and more importantly, to correlate

77   this section of the STS to the Greenland ice-core chronology. Through the temporal

78   accuracy this affords, the resulting correlation can therefore reveal crucial information

79   regarding the temporal coupling between Fennoscandian ice-sheet dynamics and

80   rapid climate change.

81   Here we reassess, update and extend the 806-year long LGC from south-eastern

82   Sweden (Wohlfarth *et al.* 1998), and link for the first time the FIS recession to the

83   Greenland ice-core time scale. The existing chronology has, moreover, been

84   complemented by new geochemical data and corroborated by idealised numerical

85   modelling of ice dynamics. These help to cast light on the changes that occurred in the

86   BIL terminating sector of the FIS around the onset of the YD. Our results highlight a

87   possible linkage between changes in ice sheet behaviour associated with the drainage

88   of the BIL and abrupt changes in atmosphere-ocean circulation in the North Atlantic

89   domain.

90

91   **Study area and methods**

92   *Study area*

93   The LGC derives from sites located along the eastern edge of the southern Swedish

94   Uplands. The terrain reaches >330 m elevation above present-day sea level in the

95   south and west of our area of interest, sloping eastwards and northwards towards the

96   Baltic Sea (Fig. 1B, C). The FIS retreated broadly NW-wards across this region. Clay-

97   varve chronologies have hitherto been the primary source of information regarding

98   the pattern and timing of ice retreat (cf. Lundqvist & Wohlfarth 2001). An absence of

99   moraines across south-eastern Sweden suggests unpunctuated retreat, an exception

100   being the Vimmerby moraine that cuts across the south of our study area (Fig. 1C).

101   Fed by fairly uniform SE-ward flow, this ice-margin position has been constrained by

102   cosmogenic nuclide dating to 14 600-14 400 cal. years ago (Johnsen *et al.* 2009; Anjar

103   *et al.* 2014). There is no further evidence of a sustained ice-margin position until the

104   Middle Swedish End Moraine Zone (MSEMZ), a broad (~10-20 km) zone stretching

105   from Lake Vättern ENE across the Östergötland lowlands. Associated with the YD, the

106   MSEMZ comprises moraines, deltas and glacio-tectonised successions linked with ice

107   margin oscillations and an extremely slow rate of retreat (Kristiansson 1986; Lundqvist

108   1987).

109   Glacial lakes were impounded across south-eastern Sweden in front of the

110   retreating ice margin, both localised and linked to the much larger BIL, which was up-

111   dammed in the Baltic Sea Basin. The BIL was maintained by the ice dam across central-

112   southern Sweden and the southern Swedish uplands and the high threshold level in

113   Öresund; not until the ice margin retreated past Mt. Billingen could any drainage occur

114   (Björck 1995). A major (25 m lake-level drop) and rapid (1-2 years) drainage of the BIL,

115   and consequent opening to marine waters (Yoldia Sea stage), occurred at the end of

116   the YD when the Billingen ice dam was released (Björck & Digerfeldt 1984; Björck

117   1995; Johnson *et al.* 2013). An earlier drainage is hypothesised to have occurred at the

118   late AL-YD transition (Björck 1995; Bennike & Jensen 2013), but its magnitude and

119   dynamics are less well-constrained. Palaeo-shorelines of the BIL are evident along the

120   east and south coast of Sweden, rising to the north as a consequence of post-glacial

121   (and ongoing) glacio-isostatic rebound (see Fig. 1).

122   AL-age glacial varved-clay successions from sites close to the former highest

123   shoreline of the BIL had earlier been investigated in the provinces of Småland and

124   Östergötland (Kristiansson 1986; Wohlfarth *et al.* 1995, 1998) (Fig. 1). Most of the

125   varve thickness diagrams were obtained in a region that formed an archipelago-like

126   landscape in the western part of the large BIL (Wohlfarth *et al.* 1998). The glacial

127   varves were thus deposited in fairly shallow waters (between ~5 and 70 m) and mostly

128   within a large fjord complex (Fig. 1). Owing to isostatic uplift of the newly deglaciated

129   areas, progressive shallowing of the depositional basins along the coast and successive

130   isolation resulted in a cessation of varve deposition and replacement by homogeneous

131   clay and organic lacustrine sediments. The recently published varve chronology from

132   Gropviken (MacLeod *et al.* 2014) and the varve chronology from Sandfjärden (this

133   study), ~50 km farther to the east, derive from sites that were located directly south

134   of the YD ice margin (Fig. 1) and at a former BIL water depth of approximately 100 m

135   (Brunnberg 1995).

136

137   *Varve and ^{14}C chronologies*

138   The original master chronology for Småland/Östergötland (the LGC) is a composite

139   chronology of 806 varve years (Wohlfarth *et al.* 1998; Wohlfarth & Possnert 2000),

140   which is based on the visual linking of common and distinct sedimentological features

141   in 55 varve diagrams (Figs. 1, 2). These correlations are corroborated by cross-

142   correlation analysis (Holmquist & Wohlfarth 1998). The chronology from Gropviken is

143   a 710 varve-year long record, which contains the Vedde Ash isochrone (MacLeod *et*

144   *al.* 2014). The chronology from Sandfjärden is a 623 varve-year long record (Fig. 1C).

145   AMS radiocarbon measurements that had been published earlier for selected

146   sites of the LGC (Wohlfarth *et al.* 1998; Wohlfarth & Possnert 2000) are here used to

147   verify the internal consistency of the new composite varve chronology (Table 1). To

148   provide the most reliable ^{14}C-based chronology, we selected only those ^{14}C

149   measurements that had been made on terrestrial plant macrofossil remains and we

150   disregarded dates that were associated with unidentified and reworked plant material

151   or had analytical errors of >250 years (Wohlfarth *et al.* 1998; Wohlfarth & Possnert

152   2000).

153   Based on Bayesian wiggle-match modelling using OxCal4.2 (Bronk Ramsey

154   2010), these ^{14}C dates were used to find the most likely possible placement of the LGC

155   on the IntCal13 radiocarbon calibration curve (Reimer *et al.* 2013). Outlying dates

156   were detected by the software applying the 'Outlier Analysis' and discarded until a

157   satisfactory and coherent age model was generated as defined by a high model

158   agreement with values higher than a threshold of 60% (Bronk Ramsey 2009).

159

160   *New cores: fieldwork, dating and elemental analyses*

161   A new sediment succession from Lake Gummetorpasjön, which was previously

162   investigated by Wohlfarth *et al.* (1998), was cored in March 2015 (Fig. 1), with the

163   purpose of performing geochemical analysis. Parallel sediment cores were collected

164   using a 1-m long Russian corer with diameters of 10 and 7.5 cm, obtaining 50 cm

165   overlapping sections.

166   Correlation to the previously established LGC chronology (Wohlfarth *et al.* 1998)

167   was carried out employing three distinct colour and varve thickness changes that were

168   identified by Wohlfarth *et al.* (1998). The marker layers, which occur 115 and 108

169   varve years apart from each other, are present in the majority of the varve diagrams

170   that compose the LGC, including Gummetorpajön (see discussion below). This allowed

171   the new XRF profiles to be placed unequivocally within the existing chronology.

172   The new Gummetorpasjön sediment cores were scanned at the Department of

173   Geological Sciences at Stockholm University using an ITRAX XRF Core Scanner from

174   Cox Analytical System (Gothenburg, Sweden) to detect chemical changes and signals

175   relating to summer and winter layers. Radiographic images were generated using a

176   Mo tube set at 55 kV and 50 mA with a step size of 200 µm and a dwell time of 400

177   ms. XRF data were acquired using a Mo tube set at 30 kV and 50 mA with a step size

178   of 200 µm and a dwell time of 30 s. Based on XRF counting statistics of the new

179   Gummetorpasjön clay-varve record, reliable data were obtained for 21 elements with

180   signals well above the instrumental noise threshold making it unnecessary to

181   normalize the peak area data to the scattering. Relative changes in peak areas of

182   elemental data were therefore used to construct ratio profiles from selected

183   elements, i.e. Zr, Rb, Fe and Ca. Elemental XRF core scanning profiles were used as

184   indicators of changes in sediment transfer rates and grain size mediated by local ice-

185   mass turnover within the fjord system.

186

187   **Results and discussion**

188   *Reconstruction of the new Lateglacial varve chronology*

189   To anchor the LGC to the chronology of Gropviken, which contains the Vedde Ash, we

190   approached the alignment systematically (see below), initially adopting Kristiansson's

191   (1986) original time scale.

192   The first step taken for correlating the Gropviken varve thickness diagram and

193   each one of the diagrams composing the LGC was to search for statistically significant

194   cross-correlations between the successions, though this proved unsuccessful due to

195   substantial differences in varve thicknesses.

196   We therefore introduced an additional alignment step by bridging Gropviken's

197   chronology and the LGC using the Sandfjärden floating varve chronology from the

198   northern sector of Östergötland (Fig. 1C). The cross-correlation of varve thickness

199   diagrams from Gropviken and Sandfjärden provided a statistically significant match (r

200   = 0.61, signal-to-noise ratio z = 7.7, p = 0.99) that enabled us to extend the varve

201   chronology to the northern sector of Östergötland (Fig. 3).

202   In a next step we linked the Sandfjärden chronology to the LGC. However, cross-

203   correlations alone could not directly link the two chronologies together. The

204   chronologies were therefore aligned via identification of three common markers, i.e.

205   two colour changes at local varve years 2060 and 2169, and a characteristic thick varve

206   horizon at local varve year 2060 (Fig. 3). This technique (e.g. Palmer *et al.* 2010)

207   provided satisfactorily fits between the successions.

208   To provide an independent test of the alignment between the LGC and

209   Gropviken's chronology, we employed an independent ^{14}C dating method (Fig. 4). The

210   LGC is supported by AMS radiocarbon measurements (Wohlfarth *et al.* 1998;

211   Wohlfarth & Possnert 2000), whereas the Vedde Ash has been precisely radiocarbon

212   dated in lake sediment records from western Norway (Lohne *et al.* 2013). The LGC was

213   anchored to the IntCal13 radiocarbon calibration curve using a Bayesian wiggle-

214   matching model based on eight radiocarbon dates. Using the calibrated age of the

215   Vedde Ash and the most likely placement of the LGC on the IntCal13 time scale,

216   respectively, we were able to calculate the offset between the chronology of

217   Gropviken and the LGC, and compare the results with the offset previously obtained

218   from the alignment approach. The offsets resulting from the two methods,

219   respectively, strongly agree with each other (-1353 years using the alignment versus -

220   1359 using wiggle-matching; Fig. 4), which indicates that the relative placement

221   between the northern and southern chronologies is coherent and reliable.

222

Age error evaluation of the Lateglacial varve chronology

The excellent correlation among the 55 varve diagrams that compose the original LGC suggests no or minimal counting errors and laterally continuous varve accumulation over this sector of Småland/Östergötland (Wohlfarth *et al.* 1998). An example of such region-wide chronological consistency is demonstrated by the precision of varve counts in relation to the interval spanning the three marker horizons utilized to link the original LGC to Sandfjärden's chronology (<1% difference).

The independent ^{14}C dating approach described in section above provides a means to verify the chronological accuracy over a large interval of the LGC, demonstrating that contributions to uncertainty from undetected systematic errors in the varve layer identification process is minimal (Fig. 4). This is also substantiated by the similarity between the inferred varve age and the unmodelled ^{14}C-calibrated curve (Fig. 4). Moreover, the biostratigraphic boundary of the AL-YD transition, which has been identified in the pollen stratigraphy from Gummetorpasjön (Björck 1999), provides an additional chronostratigraphic constraint that confirms the internal consistency of the LGC. Indeed, even considering the low-resolution pollen sampling (Björck 1999), the estimated ^{14}C-calibrated age of this regionally isochronous marker in the varve stratigraphy falls within the 1σ range of the AL-YD pollen zone boundary observed in some of the most robustly constrained radiocarbon-dated regional records (Muschitiello & Wohlfarth 2015).

We are confident that an overall uncertainty (entailing precision and accuracy) of ±0.5% (2σ) is an over-conservative estimate for the unified chronology. This is based on, *i*) the general lack of disturbed or suspicious intervals and the good preservation

246 of the varves in all the LGC profiles (Wohlfarth *et al.* 1998), *ii*) the evenly high

247 correlation among numerous adjacent and distal sites (Wohlfarth *et al.* 1998), and *iii*)

248 the internal chronological consistency determined via independent dating

249 approaches. This is realistic given that the error that accompanies most varve

250 chronologies with well-developed and undisturbed successions displaying little

251 variations between alternate counts does not exceed ±1% (Zolitschka *et al.* 2015).

252

253 *Synchronization to Greenland Ice-Core Chronology 2005 and varve stratigraphy*

254 Our new LGC extends over 1257±3 varve years (1σ) and covers the interval from the

255 regional late AL pollen zone to the regional late YD pollen zone. The chronology is

256 based on 57 varve-thickness diagrams, which were compiled to form one unified

257 record of mean varve thickness (Fig. 5). The supporting ^{14}C-based age model enables

258 us to secure the new LGC on the IntCal13 time scale. Critically, we are also now able

259 to synchronize the LGC record with the Greenland Ice-Core Chronology 2005

260 (Rasmussen *et al.* 2006; after converting the b2k age [before the year 2000] into BP

261 [before 1950 AD], hereafter GICC05 years BP) via the Vedde Ash time marker (Fig. 5).

262 This allows us, for the first time, to directly compare the dynamics of the FIS to the

263 Greenland ice-core event stratigraphy.

264 Although there are numerous distinct events with exceptionally thick varves,

265 Wohlfarth *et al.* (1998) identified only three major events in their varve chronology,

266 that are recurrent in the majority of the varve diagrams. The Events, numbered 1, 2

267 and 3 (Wohlfarth *et al.* 1998), are characterised by distinct colour changes of the clay

268 varves and based on the correlation to the ice core time scale occurred at 12 847, 12

269 739 and 12 624 GICC05 years BP, within one varve year. All the events exhibit a marked

270 drop in varve thickness that lasts for a few decades. The colour change and the drop

271 in varve thickness make Event 1, 2 and 3 different from all the other anomalous varve

272 layers that can be observed in the new LGC.

273 Events 2 and 3, which are both preceded by an exceptionally thick varve, have

274 been attributed to drainages of ice-dammed lakes located west of the BIL (Wohlfarth

275 *et al.* 1998). These events are present in all varve diagrams except for Skedevi, Räfstad

276 and Kråkedal (sites 17, 20 and 21 in Fig. 1). As such, large areas above the highest

277 shoreline remained covered by stagnant ice and continued to contribute sediment

278 material to the BIL as the ice sheet retreated (Lundqvist & Wohlfarth 2001). However,

279 it remains unclear why a decrease in varve thickness accompanies all of the events.

280 Event 1 in particular, which can be observed in all the varve diagrams covering this

281 interval (Figs. 1, 2), presents the most pronounced decrease in varve thickness of the

282 entire chronology, but is not preceded by a thick varve (Fig. 5). This suggests that the

283 causes of Event 1, which can be traced for more than 25 km eastwards (from

284 Gummetorpasjön to Tynn – Wohlfarth *et al.* 1998), are potentially not just a mere

285 response to a release of high amounts of sediment material into the BIL. Moreover,

286 based on a previously published ice-rafted debris (IRD) record (Wohlfarth *et al.* 1998)

287 that accompanies the LGC (Fig. 5), it is evident that, unlike Events 2 and 3, Event 1 is

288 the only one associated with a long-term interruption (~130 varve years) in IRD

289 deposition.

290 We note that, after synchronizing the varve record to the Greenland time scale,

291 Event 1 coincides with the transition from Greenland Interstadial 1 to Greenland

292 Stadial 1 (GS-1), which is defined in NGRIP ice cores as an abrupt shift in *d*-excess that

293 took place within 2-3 years (Steffensen *et al.* 2008). The onset of GS-1 is dated to 12

294   846±69 GICC05 years BP considering 1σ age uncertainty in the GICC05 (i.e. half of the

295   total maximum counting error – MCE; Rasmussen *et al.* 2006) and Event 1 is dated to

296   12 847±2 GICC05 years BP (accounting for 1σ of the total uncertainty that

297   accompanies the LGC). This places GS-1 and Event 1 at 725±6 years and 726±2 years,

298   respectively, prior to the Vedde Ash in their respective records.

299   The temporal consistency of Event 1 relative to the start of GS-1 requires further

300   attention. In the following, we focus on the varve stratigraphic boundary identified at

301   12 847±71 GICC05 years BP by reporting and discussing the results from XRF analyses

302   on Gummetorpasjön's succession in conjunction with output from idealised ice flow

303   model simulations.

304

305   *Geochemical evidence of depositional changes at the GI-1/GS-1 transition*

306   We use Zr/Rb and Fe/Ca ratios as proxies for grain-size distribution and composition

307   (Fig. 6). Rb, which is common in several minerals, has generally low environmental

308   mobility owing to strong sorption in clay minerals. Conversely, Zr is usually found in

309   medium to coarse silts and is present in heavy minerals. In fine-grained sediments -

310   like in our clay varves, Zr/Rb is thus an ideal proxy for grain size (Dypvik & Harris 2001).

311   Like Rb, Fe absorbs onto clay and has relatively low mobility, whereas Ca can easily be

312   found in plagioclase and calcite in the sand and silt fraction (e.g. Johnson *et al.* 2013).

313   Thus, Fe/Ca can be used here as an additional indicator for grain size.

314   The XRF data profiles entirely resolve seasonal varves associated with summer

315   and winter accumulation, with summer laminae generally characterised by larger

316   grain sizes as compared to winter laminae (Fig. 6). The XRF stratigraphies consistently

317   show a decrease in grain size 18-19 varve years before Event 1 at 12 847 GICC05 years

318   BP (Fig. 6). At 12 847 GICC05 years BP the ratio values abruptly shift indicating a

319   change towards coarser grain sizes. The shift takes place within one varve year, after

320   which the geochemical parameters indicate that depositional conditions directly enter

321   into a new stable state for a period that lasted 57-58 varve years (Fig. 6).

322   We infer increased sediment supply of fine sediments during the two decades

323   preceding Event 1, followed by a marked slowdown of sediment transfer and increase

324   in grain size at 12847 GICC05 years BP. This is coeval with a distinct drop in varve

325   thickness and disappearance of IRD (Fig. 5). The rapid change in varve thickness and

326   grain size suggest a potential large-scale shift in the lake circulation regime and/or

327   changes to how sediments are supplied to the lake.

328   Stabilisation of the ice sheet's calving margin could achieve the observed

329   changes in IRD delivery. Increased stability can be driven by glacio-isostatic rebound

330   of the crust and commensurate reduction in the proglacial water depth (Gomez *et al.*

331   2010), though its gradual nature cannot explain the abrupt sedimentation changes

332   observed in the LGC records. Rather, we suggest that a rapid fall of the BIL water level,

333   reducing calving margin buoyancy, and therefore calving, acted to abruptly decrease

334   iceberg calving flux from the ice margin.

335   The coupling between a rapid lowering of the BIL and a general decrease in varve

336   thickness together with interruption of IRD deposition has been suggested for the final

337   drainage of the BIL around the YD-Preboreal transition (Andrén *et al.* 1999, 2002). We

338   therefore argue that the evidence in the LGC and in our geochemical records

339   associated with Event 1 represent a late AL drainage of the BIL (Björck 1995). This

340   would be caused by a recession of the southern margin of the FIS beyond the lake

341   outlet. In the following, we explore the implications of this hypothesis by means of

342   simulations from a simple ice flow/calving model.

343

344   *Ice-sheet response to Baltic Ice Lake drainage*

345   A series of experiments simulating a highly idealised glacier calving margin were

346   undertaken using a well-established one-dimensional flow-line numerical model (Nick

347   *et al.* 2010) and applying a simple floatation based calving law (Vieli *et al.* 2001). These

348   were conducted to investigate changes in calving rate and terminus position following

349   a drop in lake level for a flat-bedded ice sheet. These experiments do not seek to

350   directly simulate the ice draining into the BIL, but rather illustrate the potential

351   dynamic response of an ice sheet that experiences a drop in its proglacial lake level.

352   The specifics of the model are discussed in detail elsewhere (e.g. Nick *et al.* 2010), with

353   relevant input parameters shown in Table 2.

354   The model is used to investigate calving and terminus response with respect to

355   three variables: basal roughness, initial bed depth, and size of lake-level drop. Three

356   basal roughness scenarios were tested, chosen to represent a smooth, medium and

357   rough sliding scenarios, with values defined within the range of those used for

358   contemporary Greenland modelling studies (e.g. Nick *et al.* 2013; Lea *et al.* 2014a, b).

359   Three initial bed elevations were also chosen, equivalent to the mean, 25th and 75th

360   percentile values of a transect spanning an estimated pre-YD ice margin, isostatically

361   depressed according to the Ice5G model (Peltier 2004). Finally, three different lake-

362   level drops were simulated (10, 20 and 30 m), based on current estimates of the

363   magnitude of the hypothesized pre-YD BIL drainage (Björck 1995; Bennike & Jensen

364   2013).

365   Results of highly idealised numerical model experiments investigating calving

366   and terminus behaviour are shown in Fig. 7. These demonstrate that in all cases a drop

367   in lake level would cause both a reduction in calving compared to the pre-drainage

368   iceberg flux and an advance of the ice-calving terminus. However, the magnitude of

369   these changes, ranging from 10% to 45%, is highly dependent on the initial lake depth

370   and size of the lake drop. While changes in calving are broadly unaffected by the basal

371   conditions of the ice stream, Fig. 7 also shows that rougher bed conditions limit how

372   far the glacier calving margin can advance following a lake level drop (though it should

373   be emphasised that these should not be equated to estimates of actual advance

374   distances of FIS following lake drainage).

375   The results provide evidence that the proportional reduction in calving rates will

376   have been greatest in shallow areas of the BIL. Larger drops in lake level result in

377   greater proportional decreases in calving flux, as is consistent with the floatation

378   calving law employed in the model. However, these larger drops would also increase

379   the range of calving response between shallow and deeper areas of the BIL

380   terminating sectors of FIS.

381   Model results suggest that the BIL terminating sectors of the FIS will have

382   experienced a decrease in calving flux due to decreased buoyancy (and hence

383   stabilisation) of the ice margin. Although calving rates will have responded almost

384   instantaneously to a drop in lake level, this is likely to only impact IRD frequency (as

385   identified) rather than the deposition of finer grained sediments on a lake-wide scale.

386   By itself, this can only partially explain the observed drop in IRD frequency, though it

387   is worth noting that a thinner calving margin would also produce smaller, and

388   therefore less long-lived icebergs. Faster melting icebergs would therefore decrease

389   the probability of IRD deposition in ice distal/sheltered parts of the post-drainage BIL.

390   A further consideration is that changes in lake circulation resulting from the drop in

391   BIL may have caused debris-laden icebergs to be diverted elsewhere from the coring

392   sites.

393   The presence of thinner varves following the drainage suggests that reworking

394   of material from newly exposed areas of the former lake bed did not result in

395   significant sediment supply into the lake basin. We therefore hypothesise that the

396   shift in observed sedimentation rates resulted from a rapid change in the delivery rate

397   of subglacially derived material to the lake. However, further investigation regarding

398   the major sediment sources for the varves would be required for this to be fully

399   substantiated.

400

401   *The first drainage of the Baltic Ice Lake*

402   During the latter part of the AL, rapid deglaciation of the southern FIS margin near Mt.

403   Billingen - in the south-central Swedish low-land area (Fig. 1B) – is thought to have

404   generated a spillway system that connected the BIL to the sea in the west (e.g. Björck

405   & Möller 1987; Björck 1995; Lundqvist & Wohlfarth 2001). A rapid retreat of the FIS

406   west of the outlet resulted in a 5-10 m lowering of the BIL (Björck 1995) also referred

407   to as the first drainage of the BIL.

408   Although this drainage hypothesis has long been debated, new reconstructions

409   support the occurrence of a late AL connection between the BIL and the North Atlantic

410   (Swärd *et al.* 2015) and a significant drop of the BIL water level at this time (Bennike

411   & Jensen 2013). Shore displacement curves from Hunneberg, west of Mt. Billingen,

412   provide a detailed framework for the timing of the deglaciation near the outlet and

413   the freshwater connection to the sea (e.g. Björck & Digerfeldt 1982a, b). The published

414   radiocarbon dates associated with the shoreline reconstructions have recently been

415   re-calibrated and combined using a Bayesian framework (Muschitiello *et al.* in press).

416   The radiocarbon dates indicate lake isolations from the sea near 11 000 ^{14}C years BP

417   (~□□□□□□□□□□□□□.□□ea□s□□□), a result of the deglaciation north of Mt. Billingen

418   (Björck & Digerfeldt 1982a, b). Therefore, the dates provide a chronological estimate

419   of the opening of the outlet at Mt. Billingen.

420   The combined age probability of the radiocarbon dates associated with lake

421   isolations has been compared to the age estimate of Event 1 derived from the

422   radiocarbon-based age model that underpins the LGC (Fig. 8). The two independent

423   age estimates, based on wiggle-matching and on radiocarbon calibration, are

424   remarkably similar (12867±66 cal. years BP for the opening of the outlet at Mt.

425   Billingen versus 12876±22 cal. years BP for Event 1). The good chronological

426   correspondence supports our hypothesis of late AL drainage of the BIL synchronous

427   with the start of GS-1 in the Greenland ice core chronology. Furthermore, the

428   observed offset of 30±22 years (1σ) between the GICC05 and the IntCal13 time scales

429   at the transition into GS-1 (Fig. 8) compares well with an offset of 40±30 years (1σ)

430   estimated with other independent methods of time-scale synchronization (Muscheler

431   *et al.* 2014).

432   We suggest that Event 1 can provide a precise chronological tie point that can

433   facilitate regional correlations for future varve reconstructions. In addition, this

434   stratigraphic marker - and more broadly any direct evidence of the first drainage of

435   the BIL - can potentially be used as an isochronous horizon to link records from the

436 Baltic Sea, southern Sweden and the eastern sector of the North Sea downstream of

437 the drainage route.

438

439 *Palaeoclimatic implications*

440 The abrupt shift in *d*-excess values that marks the onset of GS-1 in the NGRIP ice cores

441 (Steffensen *et al.* 2008) can be ascribed to a large southward shift of the marine

442 moisture source for Greenland precipitation (Pfahl & Sodemann 2014) driven by a

443 southward displacement of the North Atlantic westerly winds (Muschitiello *et al.* in

444 press). It has been hypothesised that such an abrupt southward diversion of the

445 westerly winds could have been triggered by a comparably abrupt westward

446 expansion of sea ice in the Nordic Seas (Muschitiello *et al.* in press). However, the

447 driving forces behind this putative swift growth of regional sea ice are still not entirely

448 discerned.

449   A catastrophic drainage of freshwater from the BIL can provide a plausible

450 explanation for a westward migration of sea ice in the Nordic Seas, and especially for

451 its abruptness, thereby providing a physical mechanism and timing for the start of GS-

452 1. We hypothesize that a powerful surge of Baltic-sourced freshwater routed north

453 along the coast of the Norwegian Sea could have increased sea-ice production and

454 moved, to some extent, sea ice off the shelf area towards the open ocean or

455 recirculated ice in the Nordic Seas. Thus, the excess sea ice was displaced westwards

456 beyond the limits expected from local climatological growth conditions and ultimately

457 exported to the subpolar North Atlantic. This phenomenon could have induced the

458 atmospheric circulation to cross thresholds beyond which the seasonal distribution of

459 sea ice in the Nordic Seas became significantly altered, instigating a widespread

460 expansion of sea ice in the North Atlantic. Nonetheless, this explanation remains

461 speculative until more detailed climate modelling studies surrounding the

462 atmosphere-ocean response to Fennoscandian meltwater outlets can be undertaken.

463

464 **Conclusions**

465 In this study we have revaluated and extended a Swedish Lateglacial varve chronology,

466 which now forms a continuous 1257-year long record spanning the period from the

467 regional late AL to the late YD pollen zone. The chronology has been secured to the

468 GICC05 and IntCal13 absolute time scales. Correlation to the Greenland ice-core

469 framework allows us, for the first time, to compare the melting history of the FIS with

470 ice-core climate events.

471   By using geochemical analyses and ice-flow modelling simulations, we suggest

472 that in the late AL a major drop of the BIL water level associated with the first drainage

473 of the BIL occurred. The drainage took place synchronously with the start of GS-1 and

474 specifically 726±2 years prior to the deposition of the Vedde Ash as compared to

475 725±6 years observed in ice-core records. The drainage event would provide a

476 plausible physical explanation for the timing and sign of hydroclimatic shifts observed

477 in the Greenland records, while the related stratigraphic marker can serve as an

478 important chronological tie-point for future regional correlation of proxy records.

479   We hope that this study will inspire future water-hosing and eddy-resolving

480 ocean model simulations that can help to shed light on the forcing mechanisms behind

481 the rapid climate changes that took place at the inception of Greenland Stadial 1 in

482 the North Atlantic region.

483

490

491   **References**

492   Andrén, T., Björck, J. & Johnsen, S. 1999: Correlation of Swedish glacial varves with the
493   Greenland (GRIP) oxygen isotope record. *Journal of Quaternary Science 14*, 361–
494   371.

495   Andrén, T., Lindeberg, G. & Andrén, E. 2002: Evidence of the final drainage of the Baltic
496   Ice Lake and the brackish phase of the Yoldia Sea in glacial varves from the Baltic
497   Sea. *Boreas 31*, 226–238.

498   Anjar, J., Larsen, N.K., Håkansson, L., Möller, P., Linge, H., Fabel, D. & Xu, S. 2014: A
499   [10]Be-based reconstruction of the last deglaciation in southern Sweden. *Boreas*
500   *43*, 132-148.

501   Bennike, O. & Jensen, J.B. 2013: A Baltic Ice Lake lowstand of latest Allerød age in the
502   Arkona Basin, southern Baltic Sea. *Geolological Survey of Denmark and Greenland*
503   *Bulletin 28*, 17–20.

504   Björck, S. 1979: Late Weichselian stratigraphy of Blekinge, SE Sweden, and water level
505   changes in the Baltic Ice Lake. *LUNDQUA Thesis 7*, 248 pp.

506   Björck, J. 1999. The Allerød-Younger Dryas pollen zone boundary in an 800-year varve
507   chronology from southeastern Sweden. *GFF 121*, 287–292.

508   Björck, S., 1995: A review of the history of the Baltic Sea, 13.0-8.0 ka BP. *Quaternary*
509   *International 27*, 19–40.

510   Björck, S. Digerfeldt, G., 1982a: New 14C dates from Hunneberg supporting the revised
511   deglaciation chronology of the Middle Swedish end moraine zone. *GFF 103*, 395–
512   404.

513   Björck, S. Digerfeldt, G., 1982b: Late Weichselian shore displacement at Hunneberg,
514   southern Sweden, indicating complex uplift. *GFF 104*, 131–155.

515   Björck, S. & Digerfeldt, G. 1984: Climatic changes at Pleistocene/Holocene boundary
516   in the Middle Swedish End Moraine Zone, mainly inferred from stratigraphic
517   indications. In Mörner, N.A., Karlén, W. (eds): *Climatic Changes on a Yearly to*
518   *Millennial Basis*. Reidel Publishing Co., Dordrecht, pp37-56.
519
520   Björck, S. & Möller, P. 1987: Late Weichselian environmental history in southeastern
521   Sweden during the deglaciation of the Scandinavian ice sheet. *Quaternary*
522   *Research 28*, 1–37.

523   Björck, S., Cato, I., Brunnberg, L. & Strömberg, B. 1992: The clay-varve based Swedish
524   Time Scale and its relation to the Late Weichselian radiocarbon chronology. *In*
525   *The Last Deglaciation: Absolute and Radiocarbon Chronologies*, 25–44. Springer,
526   Berlin.

527   Bronk Ramsey, C. 2009: Bayesian analysis of radiocarbon dates. *Radiocarbon 51*, 337–
528   360.

529   Bronk Ramsey, C. 2010: OxCal Program, v. 4.1.7, Radiocarbon accelerator unit,
530   University of Oxford, UK.

531   Brunnberg, L. 1995: Clay-varve chronology and deglaciation during the Younger Dryas
532   and Preboreal in the easternmost part of the Middle Swedish Ice Marginal Zone.
533   *Quaternaria Series A* 2, 1-95.

534   Cato, I. 1985: The definitive connection of the Swedish geochronological time scale
535   with the present, and the new date of the zero year in Döviken, northern Sweden.
536   *Boreas 14*, 117–122.

537   Cato, I. 1987: On the definitive connection of the Swedish Time Scale with the present.
538   *Sveriges Geologiska Undersökning Ca 68.* 55 pp.

539   Cato, I. 1998: Ragnar Lidén's Postglacial Varve Chronology from the Ångermanälvan
540   Valley, Northern Sweden. *Sveriges Geologiska Undersökning Ca 88.* 82 pp.

541   Cuffey, K.M. & Paterson, W.S.B. 2010: *The physics of glaciers*. 704 pp. Butterworth-
542   Heinemann, Oxford.

543   De Geer, G. 1912: Geochronology of the last 12,000 years. *Proceedings of the*
544   *International Geological Congress 1910*, 241-253.

545   De Geer, G. 1940. Geochronologia Suecica Principles. *Kungliga Svenska*
546   *Vetenskapsakademiens Handligar, Tredje Serien Band 18, No. 6*, 367 pp.

547   Dypvik, H. & Harris, N.B. 2001: Geochemical facies analysis of fine-grained siliciclastics
548   using Th/U, Zr/Rb and (Zr+ Rb)/Sr ratios. *Chemical Geology 181*, 131–146.

549   Gomez, N., Mitrovica, J.X., Huybers, P. & Clark, P.U. 2010: Sea level as a stabilizing
550   factor for marine-ice-sheet grounding lines. *Nature Geoscience 3*, 850–853.

551   Goslar, T., Wohlfarth, B., Björck, S., Possnert, G. & Björck, J. 1999: Variations of
552   atmospheric 14C concentrations over the Alleroød-Younger Dryas transition.
553   *Climate Dynamics 15*, 29–42.

554   Holmquist, B. & Wohlfarth, B. 1998: An evaluation of the Late Weichselian Swedish
555   varve chronology based on cross-correlation analysis. *GFF 120*, 35–46.

556   Johnsen, T.F., Alexanderson, H., Fabel, D. & Freeman, S.P.H.T. 2009: New [10]Be
557   cosmogenic ages from the Vimmerby moraine confirm the timing of
558   Scandinavian Ice Sheet deglaciation in southern Sweden. *Geografiska Annaler*
559   *91A*, 113-120.

560   Johnson, M.D., Kylander, M.E., Casserstedt, L., Wiborgh, H. & Björck, S. 2013:
561   Glaciomarine varved clay in central Sweden before and after the Baltic Ice Lake
562   drainage: a further clue to the drainage events at Mt Billingen. *GFF 135*, 293-
563   307.

564   Kristiansson, J. 1986: The ice recession on the southeastern part of Sweden.
565   Stockholm, *University of Stockholm, Department of Quaternary Research, Report*
566   *7*, 133 pp.

567   Lea, J. M., Mair, D. W., Nick, F. M., Rea, B. R., Weidick, A., Kjaer, K. H., Morlighem, M.,
568   Van As, D. & Schofield, J. E. 2014: Terminus-driven retreat of a major southwest
569   Greenland tidewater glacier. *Journal of Glaciology, 60*, 333-344.

570   Lea, J.M., Mair, D.W.F., Nick, F.M., Rea, B.R., As, D.V., Morlighem, M., Nienow, P. &
571   Weidick, A. 2014: Fluctuations of a Greenlandic tidewater glacier driven by
572   changes in atmospheric forcing: observations and modelling of Kangiata
573   Nunaata Sermia, 1859–present. *The Cryosphere, 8*, 2031-2045.

574   Lohne, O.S., Mangerud, J. & Birks, H.H. 2013: Precise 14C ages of the Vedde and
575   Saksunarvatn ashes and the Younger Dryas boundaries from western Norway and
576   their comparison with the Greenland Ice Core (GICC05) chronology. *Journal of*
577   *Quaternary Science 28*, 490–500.

578   Lundqvist, J. 1987: Glaciodynamics of the Younger Dryas marginal zone in Scandinavia.
579   Implications of a revised glaciation model. *Geografiska Annaler 69A*, 305-319.
580
581   Lundqvist, J. & Wohlfarth, B. 2001: Timing and east–west correlation of south Swedish
582   ice marginal lines during the Late Weichselian. *Quaternary Science Reviews 20*,
583   1127–1148.

584   Macleod, A., Brunnberg, L., Wastegård, S., Hang, T. & Matthews, I.P. 2014: Lateglacial
585   cryptotephra detected within clay varves in Östergötland, south-east Sweden.
586   *Journal of Quaternary Science 29*, 605–609.

587   Muscheler, R., Adolphi, F. & Knudsen, M.F. 2014: Assessing the differences between
588   the IntCal and Greenland ice-core time scales for the last 14,000 years via the
589   common cosmogenic radionuclide variations. *Quaternary Science Reviews 106*,
590   81-87.

591   Muschitiello, F. & Wohlfarth, B. 2015: Time-transgressive environmental shifts across
592   Northern Europe at the onset of the Younger Dryas. *Quaternary Science Reviews*
593   *109*, 49–56.

594   Muschitiello, F., Pausata, F.S.R., Watson, J.E., Smittenberg, R.H., Salih, A.A.M., Brooks,
595   S.J., Whitehouse, N.J. Karlatou-Charalampopoulou, A. & Wohlfarth, B. in press:
596   Fennoscandian freshwater control on Greenland hydroclimate shifts at the
597   onset of the Younger Dryas. *Nature Communications.*

598   Nick, F.M., Van der Veen, C.J., Vieli, A. & Benn, D.I. 2010: A physically based calving
599   model applied to marine outlet glaciers and implications for the glacier
600   dynamics. *Journal of Glaciology, 56*, 781-794.

601   Nick, F.M., Vieli, A., Andersen, M.L., Joughin, I., Payne, A., Edwards, T.L. & van de Wal,
602   R.S. 2013: Future sea-level rise from Greenland/'s main outlet glaciers in a
603   warming climate. *Nature, 497*, 235-238.

604   Palmer, A.P., Rose, J., Lowe, J.J. & MacLeod, A. 2010: Annually resolved events of
605   Younger Dryas glaciation in Lochaber (Glen Roy and Glen Spean), Western
606   Scottish Highlands. *Journal of Quaternary Science, 25*, 581-596.

607   Peltier, W.R. 2004: Global glacial isostasy and the surface of the ice-age Earth: the ICE-
608   5G (VM2) model and GRACE. *Annual Reviews of Earth and Planetary Sciences 32*,
609   111–149.

610   Pfahl, S. & Sodemann, H. 2014: What controls deuterium excess in global
611   precipitation? *Climate of the Past 10*, 771–781.

612   Rasmussen, S.O., Andersen, K.K., Svensson, A.M., Steffensen, J.P., Vinther, B.M.,
613   Clausen, H.B., Siggaard-Andersen, M.L., Johnsen, S.J., Larsen, L.B., Dahl-Jensen,
614   D., Bigler, M., Röthlisberger, R., Fischer, H., Goto-Azuma, K., Hansson, M.E. &
615   Ruth, U. 2006: A new Greenland ice core chronology for the last glacial
616   termination. *Journal of Geophysical Research: Atmospheres 111*, D061202.

617   Reimer, P.J., Bard, E., Bayliss, A., Beck, J.W., Blackwell, P.G., Bronk Ramsey, C., Buck,
618   C.E., Cheng, H., Edwards, R.L. & Friedrich, M. 2013: IntCal13 and Marine13
619   radiocarbon age calibration curves 0-50,000 years cal BP. *Radiocarbon 55*,1869-
620   1887.

621   Steffensen, J.P., Andersen, K.K., Bigler, M., Clausen, H.B., Dahl-Jensen, D., Fischer, H.,
622   Goto-Azuma, K., Hansson, M., Johnsen, S.J., Jouzel, J., Masson-Delmotte, V.,
623   Popp, T., Rasmussen, S.O., Rothlisberger, R., Ruth, U., Stauffer, B., Siggaard-
624   Andersen, M.-L., Sveinbjrnsdottir, A.E., Svensson, A. & White, J.W.C. 2008: High-

625   Resolution Greenland Ice Core Data Show Abrupt Climate Change Happens in
626   Few Years. *Science 321*, 680–684.

627   Swärd, H., O´Regan, M., Ampel, L., Ananyev, R., Chernykh, D., Flodén, T., Greenwood,
628   S.L., Kylander, M.E., Mörth, C.M., Preto, P. & Jakobsson, M. 2015: Regional
629   deglaciation and postglacial lake development as reflected in a 74 m sedimentary
630   record from Lake Vättern, southern Sweden. *GFF*, 1-19.

631   Vieli, A., Funk, M. & Blatter, H. 2001: Flow dynamics of tidewater glaciers: a numerical
632   modelling approach. *Journal of Glaciology, 47*, 595-606.

633   Wohlfarth, B. 1996: The chronology of the last termination: a review of radiocarbon-
634   dated, high-resolution terrestrial stratigraphies. *Quaternary Science Reviews 15*,
635   267–284.

636   Wohlfarth, B. & Possnert, G. 2000: AMS radiocarbon measurements from the Swedish
637   varved clays. *Radiocarbon 42*, 323–334.

638   Wohlfarth, B., Björck, S., Possnert, G., Lemdahl, G., Brunnberg, L., Ising, J., Olsson, S.
639   & Svensson, N.-O. 1993: AMS dating Swedish varved clays of the last
640   glacial/interglacial transition and the potential/difficulties of calibrating Late
641   Weichselian "absolute"chronologies. *Boreas 22*, 113–128.

642   Wohlfarth, B., Björck, S., Holmqvist, B., Lemdahl, G. & Ising, J. 1994: Ice recession and
643   depositional environment in the Blekinge archipelago of the Baltic Ice Lake. *GFF*
644   *116*, 3–12.

645   Wohlfarth, B., Björck, S. & Possnert, G. 1995: The Swedish time scale; a potential
646   calibration tool for the radiocarbon time scale during the late Weichselian.
647   *Radiocarbon 37*, 347–359.

648   Wohlfarth, B., Björck, S., Cato, I. & Possnert, G. 1997: A new middle Holocene varve
649   diagram from the river Ångermanälven, northern Sweden: indications for a
650   possible error in the Holocene varve chronology. *Boreas 26*, 347–353.

651   Wohlfarth, B., Björck, S., Possnert, G. & Holmquist, A.N.D.B. 1998: 800-year long,
652   radiocarbon-dated varve chronology from south-eastern Sweden. *Boreas 27*,
653   243-258.

654   Zolitschka, B., Francus, P., Ojala, A.E.K. & Schimmelmann, A. 2015: Varves in lake
655   sediments – a review. *Quaternary Science Reviews 117*, 1–41.

656

657   **Figure and Table captions**

Figure 1. A. Locations of southern Sweden and NGRIP ice cores. B, C. Location of the sites used to construct the new Lateglacial varve chronology in southern Sweden. Black circles refer to sites studied by Wohlfarth *et al.* (1995). Red circles refer to sites studied by Kristiansson (1986). Blue numbers indicate the sites where the depositional Event 1 (Wohlfarth *et al.* 1998) was identified (see text for details). Note that Event 1 can be observed in all the varve diagrams that cover the related time interval. Ice marginal positions are based on Lundqvist & Wohlfarth (2001) and visual interpretation of moraine positions from the LiDAR-based topography. The southernmost ice marginal line refers to the Younger Dryas ice limit (YD). The northernmost ice marginal line refers to the ice limit shortly before the last drainage of the Baltic Ice Lake. Highest shoreline data from Geological Survey of Sweden on a colour scale graded according to present-day elevation (highest lake position was time-transgressive: yellow to red). 1= Bjärka-Säby; 2= Skaggebo; 3= Nåtvin; 4= Vårdnäs; 5= Järnlunden/Stensvassa; 6= Limmern; 7= Storsjön; 8, 9= Mjölsjön; 10= Järnlunden/Sonebo; 11= Bjärsjön; 12, 13, 14= Glottern; 15= Eknäs; 16= Rimforsa; 17= Skedevi; 18= Ytterbo; 19= Räfstad; 20= Äfsinge; 21= Åsunden/Krågedal; 22= Vigerstad; 23= Hägerstad; 24= Rävantorpasjön; 25= Lillsjön; 26= Drättinge; 27= Boda; 28= Årteryd; 29= Utdala; 30= Stjärnevik; 31= Tynn/Tyllinge; 32= Tynn/Draboviken; 33= Nedre Emmaren; 34= Bjuggö; 35= Kärra; 36= Lövdalen; 37= Gumhem; 38= Långebro; 39, 40, 41= Hargsjön ; 42= Hargsjön 1; 43= Kisa; 44, 45= Adlerskogsjön; 46, 47= Gummetorpasjön ; 48= Kristineberg; 49= Greby; 50= Åby; 51= Väsby; 52= Dråpetorp; 53= Brunebo; 54= Järpekullen; 55= Kåreda. The location of Gropviken and Sandfjärden is also shown (green circles). LiDAR topography © Lantmäteriet.

682   **Figure 2.** Length of the varve-thickness diagrams used to construct the chronology

683   presented in Wohlfarth *et al.* (1998) and displayed on the local varve time scale

684   proposed by Kristiansson (1986). The chronology is based on diagrams studied by

685   Kristiansson (1986) and Wohlfarth *et al.* (1995), which were visually and statistically

686   cross-correlated with each other (Holmqvist & Wohlfarth 1998). Numbers refer to the

687   original coding scheme used by Holmqvist & Wohlfarth (1998). The three major

688   depositional events identified by Wohlfarth *et al.* (1998) are also shown at the bottom.

689   The events are characterised by distinct colour changes of the clay varves and a

690   marked drop in varve thickness that last for a few decades (see text for details).

691

692   **Figure 3.** Varve-width and stratigraphic alignment of the varve records forming the

693   new composite Lateglacial varve chronology from Småland/Östergötland presented

694   on the local varve time scale (Kristiansson 1986). The two northernmost successions

695   of Gropviken and Sandfjärden were first cross-correlated with each other. Prior to

696   cross-correlation time series were detrended applying a 16th degree Fourier

697   transform, filtered using a 3-year moving average and removing the first 10 bottom

698   varves, and normalized by their standard deviation. The correlation coefficient (*r*) and

699   statistics (signal-to-noise ratio *z* and *p*-value) between the individual records are given

700   in the graph. Sandfjärden's chronology was correlated to the 806-year long master

701   chronology (Wohlfarth *et al.* 1998) via common stratigraphic markers (two marked

702   colour changes and an exceptionally thick varve layer). The master chronology

703   presented here was filtered by removing the first 10 bottom varves of each varve

704   diagram.

705

706   **Figure 4.** Top panel: Wiggle-matching age model of the Lateglacial varve chronology

707   (LGC) and verification of its placement relative to the chronology of Gropviken

708   containing the Vedde Ash time marker. The age model of the LGC is based on

709   radiocarbon dates from selected terrestrial plant macrofossils previously published in

710   Wohlfarth *et al.* (1998) (blue crosses; Table 1). A radiocarbon-based calendar age for

711   the Vedde Ash in Gropviken (red cross) was assigned using precise estimates from

712   Lake Kråkenes in Western Norway (Lohne *et al.* 2013). The most likely position of each

713   radiocarbon estimate on the modelled IntCal13 calibration curve (grey; Reimer *et al.*

714   2013) is shown. In the upper-left panel is presented the comparison of the estimated

715   offsets between the LGC and Gropviken using cross-correlation and radiocarbon-

716   based methods, respectively (see text for details). The goodness of the placement of

717   the LGC relative to Gropviken is further confirmed by the position of the Allerød-

718   Younger Dryas pollen-defined boundary on the master chronology, which is consistent

719   with previously reported age estimates for this biostratigraphic event (Muschitiello &

720   Wohlfarth 2015). The probability distribution functions of the most likely placement

721   on the IntCal13 time scale of the LGC and the Vedde Ash, respectively, are also shown

722   together with their 2 sigma standard error. Bottom panel: Plot showing varve-age

723   against depth (blue dots and dashed line). The varve-age-depth relationship is

724   compared to the calibrated ^{14}C curve based on the unmodelled radiocarbon

725   measurements listed in Table 1 (black dots). Bars indicate 2 sigma standard error

726   associated with each measurement and the additional varve-age error related to

727   macrofossil sampling (Wohlfarth *et al.* 1998). The varve-age scale is based on

728   synchronization to the IntCal13 time scale using the radiocarbon-based age estimate

729   of the Vedde Ash (red dot).

730

731 **Figure 5.** The new Lateglacial varve chronology presented as a unified record of mean

732 varve thickness and plotted against the GICC05 time scale (after converting the b2k

733 age into BP) and IntCal13 time scale after synchronization via the Vedde Ash isochron

734 and wiggle-match modelling, respectively. Mean annual varve widths are displayed

735 together with a 10-year running average (red line). The chronology is plotted with a

736 record of ice-rafted mineral debris (blue histogram) formerly published in Wohlfarth

737 *et al.* (1998). The vertical dashed lines indicate the interval analysed for ice-rafted

738 debris grains. The three major depositional events identified by Wohlfarth *et al.* (1998)

739 are also displayed. The green bar shows the timing of the regional AL-YD pollen

740 boundary as defined in the Lateglacial varve chronology (Björck, 1999), which lags the

741 onset of Greenland Stadial 1 by ~150 years.

742

743 **Figure 6.** XRF elemental results from new Gummetorpasjön's varve records. All data

744 are smoothed using a 10-point running mean to facilitate visualization (black line). For

745 reference, the XRF data are presented with the optical and radiographic

746 stratigraphies. The stratigraphic transition referred to as Event 1 and synchronous

747 with the start of Greenland Stadial 1 in ice-core records is highlighted by the red

748 dashed line. The XRF elemental profiles consistently show relative changes in ratio

749 values 18-19 varve years before Event 1 (shaded area). Note inverse axis for Zr/Rb

750 ratios.

751

752 **Figure 7.** Results of idealised model runs showing change in calving fluxes and

753 terminus position 10 years after an instantaneous drop in lake level is applied. These

754 are shown for three different initial lake levels, and three different potential lake level

755 drops. These experiments were run for (A) low, (B) medium, and (C) high basal

756 roughness scenarios.

757

758 **Figure 8.** Calendar age of Event 1 in the new Lateglacial varve chronology relative to

759 the GICC05 and IntCal13 time scale and compared with estimated age of the start of

760 Greenland Stadial 1 in Greenland ice cores. The age of Event 1 is also compared with

761 the combined probability of a number of calibrated radiocarbon dates constraining

762 the timing of the first drainage of the Baltic Ice Lake and presented in Muschitiello *et*

763 *al.* (in press). The calibrated radiocarbon dates refer to lake isolations from the sea,

764 which indicate timing of deglaciation of the outlet system west of Mount Billingen in

765 southern Sweden, near 11 000 ^{14}C years BP (Björck and Digerfledt 1982a, b). Two dates

766 refer to isolation owing to concomitant lowering of the Baltic Ice Lake in Blekinge

767 (Björck 1979) and one refers to the timing of the Baltic Ice Lake water-level fall as

768 recorded in Arkona Basin, southern Baltic Sea (Bennike & Jensen 2013). All ages are

769 here presented with their 1 sigma uncertainty and error bars. Under the assumption

770 of synchronicity between Event 1, the first drainage of the Baltic Ice Lake and the onset

771 of Greenland Stadial 1, the estimated offset between the GICC05 (after converting the

772 b2k age into BP) and the IntCal13 time scales at the transition into Greenland Stadial

773 1 is of 30±22 years (1σ).

774

775 **Table 1.** AMS ^{14}C dates from glacilacustrine varves of the Östergötland master

776 chronology. All dates are based on selected terrestrial plant remains and used to

777 construct the Bayesian wiggle-matching age model presented in this study.
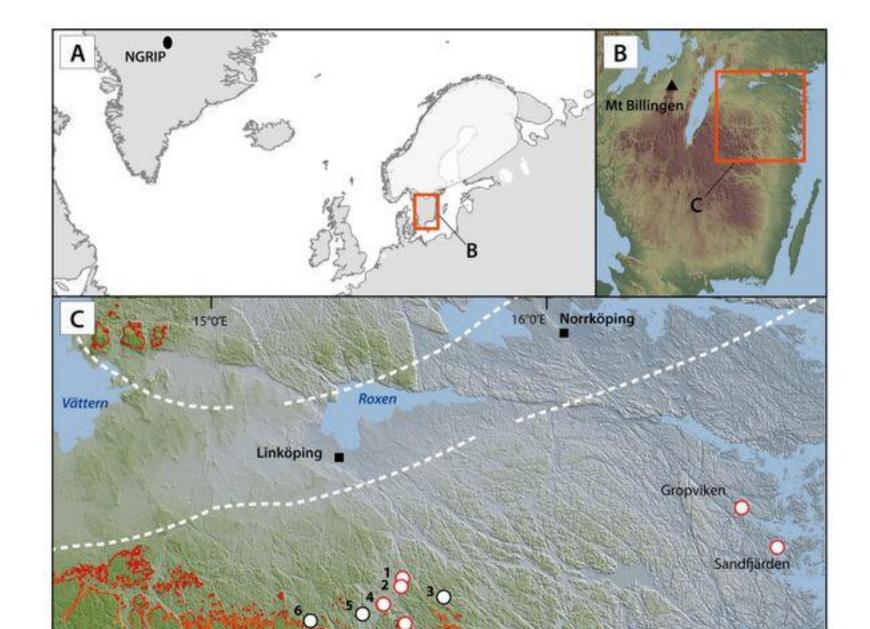
778

779   **Table 2.** Input parameters used in the ice flow/calving model experiments.

Table **Error! No sequence specified.**

Sample ID	Site	Local Varve Years	¹⁴C age (year)	¹⁴C error (1 sigma)	Used in the age model
Ua-11233	Nedre Emmaren	2221±52	10 740	240	No
Ua-10181	Gummetorpasjön	2199±32	11 450	240	No
Ua-11234	Nedre Emmaren	2146±23	10 885	250	Yes
Ua-3131	Tynn	2125±35	10 890	120	Yes
Ua-10182	Gummetorpasjön	2123±30	11 470	130	No
Ua-10183	Gummetorpasjön	2090±18	11 030	120	Yes
Ua-4358	Hargsjön	2055±50	10 980	100	Yes
Ua-10184	Gummetorpasjön	2044±16	10 970	90	Yes
Ua-2753	Hargsjön	2010±45	10 480	150	No
Ua-10185	Gummetorpasjön	2009±16	11 230	100	No
Ua-4493	Adlerskogssjön	2003±59	10 830	165	Yes
Ua-4359	Hargsjön	1973±31	10 610	110	Yes
Ua-10186	Gummetorpasjön	1968±25	11 040	110	No
Ua-10187	Gummetorpasjön	1938±4	10 420	220	Yes
Ua-4496	Glottern	1856±50	10 585	465	No

781
782
783

Table 2

Parameter/Constant	Value
Ice density – ρ_i	900 kg m^{-3}
Meltwater density – ρ_w	1000 kg m^{-3}
Proglacial water body density – ρ_p	1000 kg m^{-3}
Gravitational acceleration - g	9.8 m s^{-2}
Friction exponent - m	3
Excess floatation fraction - q	0.09
Glen's flow law exponent - n	3
Glen's flow law coefficient - A	2.93 x 10^{-17} Pa^{-3} a^{-1}
	Corresponding to -5 °C (Cuffey & Paterson, 2010)
Initial grid size	~250 m
Time step	0.005 a

784
785

Fig
Järnlunden/Stensvassa
Limmern
Järnlunden/Sonebo
Mjölsjön 2
Mjölsjön 1
Storsjön
Nåtvin
Bjärsjön
43a
42b
41
Glottern 3
Glottern 2
Glottern 1
40
39
38
Åsunden/Krågedal
Rävantorpasjön
37
36
35
Lillsjön
Hargsjön 3
Hargsjön 2
Hargsjön 1
Hargsjön 4
Adlerskogsjön 1
Adlerskogsjön 2
33
32
31
30
29
Gummetorpasjön 2
Gummetorpasjön 1
28
27
26
25
Nedre Emmaren
24
23
Tynn/Draboviken
Tynn/Tyllinge

Left panel axes: Radiocarbon years BP (y-axis); IntCal13 years (x-axis); Probability (right y-axis).

Inset: ¹⁴C wiggle matching, median offset: -1359, sigma: 45; cross-correlation offset: -1353; Offset (years) -1300 -1350 -1400; 1 sigma

Vedde Ash median age: 12066 sigma: 42

Placement of the LGC median age: 12645 sigma: 22

Gropviken; LGC; AL-YD boundary

Right panel axes: Varve years BP (based on IntCal13) (y-axis); Composite depth (arbitrary start at 10 m) (x-axis).

Vedde Ash; AL-YD boundary

	Zr/Rb	Fe/Ca	Ca/Ti
	0.0 0.4 0.8 1.2	0 20 40 60 80 100	0 2 4 6 8
	Grain size	Terrestrial input	Productivity
	+ ← → -	- ← → +	- ← → +

Depth (m)

4.0
4.1
4.2
4.3
4.4
4.5
4.6
4.7
4.8

12847 GICC05 years

12876 IntCal13 years

Low basal roughness
75 Pa m$^{-2/3}$ s$^{-1/3}$

Medium basal roughness
100 Pa m$^{-2/3}$ s$^{-1/3}$

High basal roughness
125 Pa m$^{-2/3}$ s$^{-1/3}$

Percentage change in calving flux

Distance change from prior to lake drop (m)

Initial bed elevation (m)
× -158 m
+ -198 m
● -253 m

Lake drop:
— 10 m
— 20 m
— 30 m

GICC05 years BP

GI1-GS1 transition: 12846 ± 69 GICC05 years BP
Event (1): 12847 ± 71 GICC05 years BP

GI1-GS1 transition: 725 ± 6 years from Vedde Ash
Event (1): 726 ± 2 years from Vedde ash

Event (1): 12876 ± 22 IntCal13 years
BIL drainage: 12867 ± 66 IntCal13 years